



A hindcast study of the Piedmont 1994 flood: the CIMA Research Foundation hydro-meteorological forecasting chain

Antonio Parodi¹ · Martina Lagasio¹ · Agostino N. Meroni^{1,2} · Flavio Pignone¹ · Francesco Silvestro¹ · Luca Ferraris¹

Received: 27 March 2020 / Accepted: 12 November 2020 / Published online: 10 December 2020
© The Author(s) 2020

Abstract

Between the 4th and the 6th of November 1994, Piedmont and the western part of Liguria (two regions in north-western Italy) were hit by heavy rainfalls that caused the flooding of the Po, the Tanaro rivers and several of their tributaries, causing 70 victims and the displacement of over 2000 people. At the time of the event, no early warning system was in place and the concept of hydro-meteorological forecasting chain was in its infancy, since it was still limited to a reduced number of research applications, strongly constrained by coarse-resolution modelling capabilities both on the meteorological and the hydrological sides. In this study, the skills of the high-resolution CIMA Research Foundation operational hydro-meteorological forecasting chain are tested in the Piedmont 1994 event. The chain includes a cloud-resolving numerical weather prediction (NWP) model, a stochastic rainfall down-scaling model, and a continuous distributed hydrological model. This hydro-meteorological chain is tested in a set of operational configurations, meaning that forecast products are used to initialise and force the atmospheric model at the boundaries. The set consists of four experiments with different options of the microphysical scheme, which is known to be a critical parameterisation in this kind of phenomena. Results show that all the configurations produce an adequate and timely forecast (about 2 days ahead) with realistic rainfall fields and, consequently, very good peak flow discharge curves. The added value of the high resolution of the NWP model emerges, in particular, when looking at the location of the convective part of the event, which hit the Liguria region.

Keywords Flood · Hindcast · Hydro-meteorology · WRF · Heavy orographic rainfall · Convective rain

✉ Antonio Parodi
antonio.parodi@cimafoundation.org

1 Introduction

At the beginning of November 1994, a heavy precipitation event (HPE) caused extensive flooding in Piedmont and in Liguria, two regions in northern Italy. Maximum precipitation values in excess of 200 mm caused around 6400 billion lira of damages, equivalent to roughly 3.3 billion euros, and 70 casualties (Lionetti 1996).

The Mediterranean area is frequently hit by HPEs that can trigger severe floods and flash floods, which are responsible for massive damages and, sometimes, numerous casualties (Llasat et al. 2013). Such HPEs are usually characterised by the presence of four factors: a moist low-level jet coming from the relatively warmer Mediterranean Sea; a conditionally unstable air mass; a mesoscale lifting mechanism, such as an orographic barrier; and a synoptic pattern that slowly evolves in time (Nuissier et al. 2008; Dayan et al. 2015). The fact that the Mediterranean basin is almost completely surrounded by high orography makes the conditions favourable to the development of HPEs along its coastlines.

In particular, Molini et al. (2011) distinguished two types of HPEs, according to the time-scales at which the convective instability produced by the large scale is removed by the upward motion and the subsequent precipitation. On the one hand, in type I HPEs, the convective instability is continuously consumed, and thus these events are long-lived (duration > 12 h) and widespread (more than $50 \times 50 \text{ km}^2$). On the other hand, in type II events, convective available potential energy (CAPE) builds up and, only with an appropriate trigger, an intense (< 12 h) and localised (less than $50 \times 50 \text{ km}^2$) rainfall is produced. From a forecaster standpoint, since type II events are often controlled by local forcing factors that initiate the upward motion (e.g. surface wind convergence lines, gradients in the surface heat fluxes), they are harder to predict (Fiori et al. 2017).

Concerning the Piedmont 1994 HPE, numerical studies, such as the works by Buzzi et al. (1998) and Romero et al. (1998), and observational studies, such as the work by Doswell III et al. (1998), have highlighted that the dynamics of this event was strongly controlled by the synoptic scale forcing. In particular, at 00 UTC on the 4th of November 1994, a low pressure system slightly west of Ireland was associated with a deep trough in the 500-hPa geopotential field, covering the eastern Atlantic and the western European coasts (Fig. 1a). Over southern Italy and the East European countries, instead, a ridge was in place. At the surface, a southerly pre-frontal low-level jet brought moist and unstable air from the Mediterranean Sea to the coastlines of southern France and northern Italy, impinging on the high orography of the Alpine arc. During the day, while the trough slowly moved eastward, the ridge was stationary, leading to an increase in the geopotential gradient and resulting in a slowing down of the system. On the 5th of November, this produced a slight counterclockwise rotation of the upper level trough (Fig. 1b). At the surface, the southerly jet increased with respect to the previous day because of the spatial contraction of the system due to the stationarity of the pressure high over the Balkans. The fact that the system was quasi-stationary is responsible for the high accumulated rainfall depths observed in this event. Figure 1c shows that even on the 6th of November there was a surface low-level jet bringing warm and moist air from the sea towards the orographic features of north-western Italy.

The event developed in two phases. The first phase, characterised by embedded convection, hit the southern part of Piedmont and the western part of Liguria between the 4th and 5th of November. The second one brought persistent rainfall between the 5th and 6th of November over the northern part of the region and was mainly driven by the stratiform orographic uplift (Buzzi et al. 1998), as highlighted by Monte Lema radar rainfall intensity

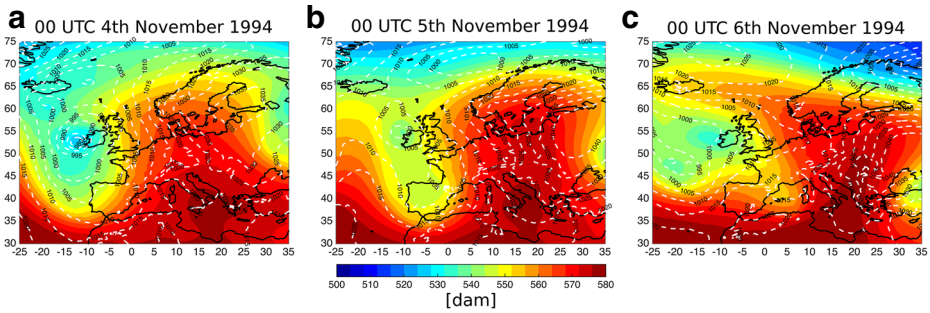


Fig. 1 500 hPa geopotential height (colours) and sea level pressure (dashed contours) on the 4th, 5th, and 6th of November 1994 at 00 UTC (panels **a**, **b**, and **c**, respectively)

observations (Fig. 2). Despite most of the rainfall was stratiform, intense convective activity embedded in the large-scale system was also observed by means of infrared and microwave satellite imagery by Boni et al. (1996).

The numerical simulations of Ferretti et al. (2000), in agreement with the previously cited works, highlighted the importance of the positive vorticity anomaly produced by the latent heat released during the airflow ascent. Notably, this was found to contribute to slowing down the eastward movement of the rain band, resulting in large accumulated rainfall values. Rotunno and Ferretti (2001) investigated the role of surface convergence produced by the differential orographic deflection of the flow, due to the presence of a horizontal moisture gradient. In fact, while a moist saturated airflow is able to overcome the orographic barrier due to its relatively low stability, a dry and unsaturated flow is blocked by the mountainous chain. Thus, an impinging flow characterised by a horizontal moisture gradient has a non-homogeneous response to the orography and surface convergence can be produced.

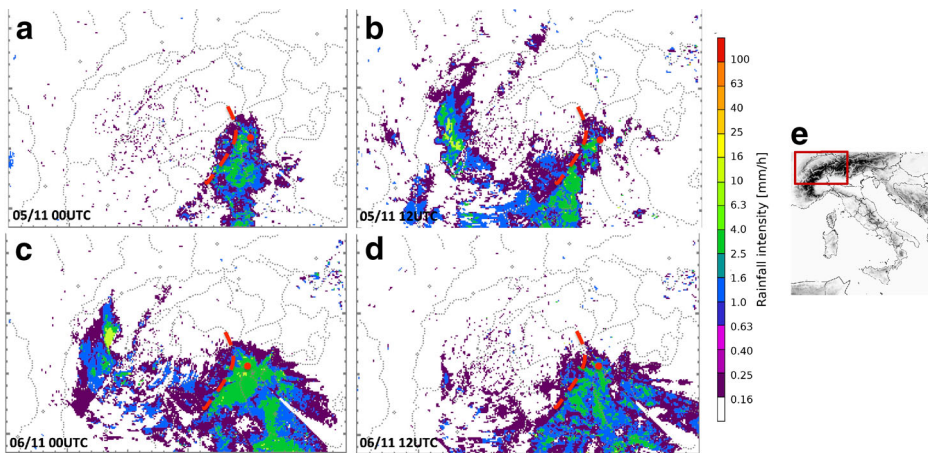


Fig. 2 Rainfall intensity (mm/h) on the 5th of November at 00 and 12 UTC (panels **a**, **b**), and on the 6th of November at 00 and 12 UTC (panels **c**, **d**) observed by the Monte Lema radar. The red marker shows the radar location, while the red dashed curve identifies the norther portion of Piedmont interested by widespread and persistent stratiform rainfall phenomena. Panel **e** shows a map of Italy with a red rectangle indicating the area covered by panels (a)–(d)

Rainfall events in regions with complex orography can be easy to simulate, when the large-scale orographic barrier is the main forcing of the ascent, but can also be very hard to forecast, especially when convection takes place. The main difficulties arise because in NWP models with typical cloud resolving resolutions, $O(1\text{ km})$, the simulated orography is smoother with respect to the real one. The simulated surface fluxes, turbulence, internal waves, and the consequent atmospheric dynamical evolution can, thus, drift from the real event resulting in a bad forecast. Since local factors can be important in the rainfall development and evolution, extensive research has been carried out, both with observational and with modelling studies, to understand the dominating mechanisms in this kind of rainfall events. As an example, the Mesoscale Alpine Programme (MAP) was performed to study HPEs in the Alpine region, motivated also by the 1994 Piedmont event (Volkert 2005; Bougeault et al. 2001).

Within the MAP project, various intensive observation periods encouraged multiple numerical experiments. For example, Chiao et al. (2004) studied the local circulation during the HPE of the 19th–21st of September 1999, observed during MAP. The conditions leading to this event were similar to those that characterised the Piedmont 1994 event. By means of numerical simulations, Chiao et al. (2004) found that in this event the Apennines Mountains and the French Alps played a minor role in determining the rainfall location. They also found that the high spatial resolution enabled them to resolve more intense convection by adding small-scale features in the orographic forcing. Interestingly, they highlighted that the surface friction played a crucial role for the deflection of the southerly flow and, by turning it off, more rainfall was produced because of stronger surface convergence, but convection was shallower, due to the reduced turbulent surface heat fluxes. This indicates how important local factors are in determining the rainfall evolution.

A fundamental element in the simulation of rainfall over complex orography is the choice of the microphysical scheme. In fact, the ratio between the terminal velocity of the different hydrometeors and the horizontal advection determines the location of the precipitation. In turn, the hydrometer terminal velocity is determined by the number of cloud condensation (and ice) nuclei, through the control on the hydrometeor size (Roe 2005). All these aspects are handled by the microphysical scheme, hence its importance. The precipitation location is also strongly controlled by the orography geometry, which, in the numerical grid of NWP models, is always smoother than in the real world. To investigate this aspect, Roe and Baker (2006) developed an intermediate model in a simplified setup with the goal of interpreting precipitation patterns in terms of the prevailing winds, several cloud microphysics properties and the dimensions of the mountain range. Their model is not suitable for comparison with the observations but it can be used to study the effects of slanting hydrometeor trajectories and mountain geometry on the precipitation pattern.

An example of numerical study to assess the role of microphysics in heavy precipitation events over complex orography, such as the Alps, in a realistic setup is the work performed by Zängl (2007a). The two HPEs considered were characterised by synoptic conditions similar to those leading to the Piedmont case. It was found that the hydrometeor terminal velocities and the height of the freezing level are important factors determining the rainfall location. These results can help to understand why in regions with such a complex orography convective activity can control the small-scale precipitation spatial variability. From an observational standpoint, these small-scale features are very hard to capture with the standard rain gauge networks because of their relatively low spatial density. Radar observations can help to detect convective structures because they are deep enough to be observed above

the orography. Zängl (2007b), by running high-resolution numerical simulations in realistic and semi-idealised configurations, studied the small-scale precipitation variability in the Alps. In particular, he found that the large-scale variable which has the strongest impact on the small-scale rainfall distribution is the wind direction. In his experiments, he also found that the large-scale wind speed influenced the rainfall intensity, while the background temperature profile modified the rainfall pattern, because of the different terminal velocities of the microphysical species.

In this work, the performances of a state-of-the-art high-resolution hydro-meteorological prediction framework are studied in the hindcast simulation of the November 1994 event in Piedmont and Liguria. The modelling chain is composed of the cascade of the Advanced Research version of the Weather Research and Forecasting (WRF-ARW) model (Skamarock et al. 2008; Powers et al. 2017), a stochastic downscaling model, RainFARM (Rebora et al. 2006), and a hydrological model, Continuum (Silvestro et al. 2013), which are all described in the next section. The overarching idea of this paper is to test whether the proposed framework, operational since 2018 at CIMA Research Foundation in support of the Italian Civil Protection Department (ICPD) and the Regional Agency for Environmental Protection of Liguria (ARPAL), would be able to forecast with adequate predictive capability the November 1994 flooding event in Piedmont and Liguria. In particular, four microphysical schemes are tested in the atmospheric model to assess the sensitivity of the full hydro-meteorological chain to this crucial parameterization.

Section 2 introduces the models and their setup used in this work. Meteorological and hydrological results are presented in Section 3, and conclusions are given in Section 4.

2 Models and experiments

2.1 Weather Research and Forecasting model

The Weather Research and Forecasting (WRF) model is a proven mesoscale numerical weather prediction system, designed to serve both operational forecasting and atmospheric research needs. It solves the fully compressible non-hydrostatic Euler equations using an Arakawa-C grid with mass-based terrain-following coordinates. It features multiple dynamical cores, a three-dimensional variational data assimilation system (3DVAR), and a software architecture allowing for computational parallelism and system extensibility. WRF is suitable for a broad spectrum of applications across scales ranging from metres to thousands of kilometres, and has been used by the authors for hydro-meteorological research applications in tropical and subtropical areas (Parodi and Tanelli 2010; Viterbo et al. 2016; Marras et al. 2017), and for mid-latitude severe weather studies (Parodi et al. 2012; Fiori et al. 2014; Viterbo et al. 2016; Fiori et al. 2017; Lagasio et al. 2017; Lagasio et al. 2019a; Lagasio et al. 2019b; Lagasio et al. 2019c; Parodi et al. 2019; Silvestro et al. 2019; Meroni et al. 2018b).

The setup used for this work has been tested and used for operational applications by CIMA Foundation for ICPD and for ARPAL, as well as in previous research works (Lagasio et al. 2019a; Lagasio et al. 2019b; Lagasio et al. 2019c): it consists of a configuration with three two-way nested domains with horizontal grid spacing of 13.5, 4.5, and 1.5 km and with 50 vertical levels (Fig. 3).

The Yonsei University scheme (Hong et al. 2006) was chosen as planetary boundary layer turbulence closure; the RRTMG shortwave and longwave schemes (Iacono et al. 2008; Mlawer et al. 1997; Iacono et al. 2000) were used for the radiative transfer computations;

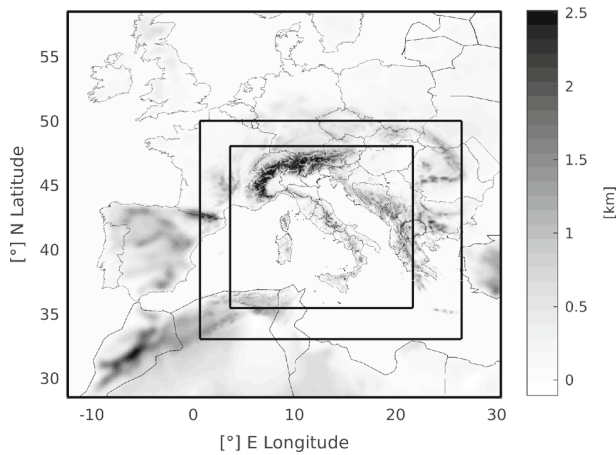


Fig. 3 WRF domains with 13.5-, 4.5-, and 1.5-km grid spacing, from the largest domain to the innermost one

and the Rapid Update Cycle (RUC) scheme was chosen as a multi-level soil model (6 levels) with higher resolution in the upper soil layer (0, 5, 20, 40, 160, 300 cm) (Smirnova et al. 1997; Smirnova et al. 2000). No cumulus scheme was activated in the two innermost domains because the grid spacing enables to explicitly resolve the convective dynamics. For consistency with the boundary conditions, the Tiedtke convection scheme (Tiedtke 1989; Zhang et al. 2011) was used in the outermost domain.

Concerning microphysics, four different schemes were considered, namely:

- WSM6 (Hong and Lim 2006, WRF Single Moment 6-class): it is a single-moment scheme with 5 species (cloud, rain, ice, snow, graupel), used in the operational configuration run by CIMA Research Foundation. It represents the mixed-phase particle terminal velocity for the snow and graupel particles by weighting their separate terminal velocity with their mixing ratio. This adds complexity to how the hydrometeor terminal velocity is treated in the model which, as discussed in the “Introduction”, might lead to significant variations in the simulated rainfall pattern;
- Goddard (Tao et al. 2001): it is a single-moment scheme with 5 species. It assures a proper water balance in the phase change of the microphysical particles with an accurate thermodynamic treatment. This scheme offers an option to choose either graupel or hail as the third class of ice (McCumber et al. 1991). In this study, the graupel has been chosen, so that the 5 species are the same as in the WSM6 option;
- Thompson (Thompson et al. 2008): it handles 5 microphysical species (the same as in the WSM6 and Goddard schemes), with a double-moment approach for cloud water, ice, and rain only. With respect to previous versions, it incorporates more sophisticated spectral bin schemes using updated look-up tables;
- Milbrandt-Yau (Milbrandt and Yau 2005a; 2005b): it is the only fully double-moment scheme used in this study and, with respect to the others, it has one extra hydrometeor, namely hail.

The difference between single- and double-moment schemes is that single-moment schemes only solve the equations for the mixing ratios (one equation for each microphysical species), while double-moment schemes also account for equations describing the

number concentration variables. Note that some schemes may be single-moment for some hydrometeors and double-moment for others, as the Thompson scheme.

Initial and hourly boundary conditions were generated by the European Centre for Medium-Range Weather Forecasts (ECMWF) on purpose for this study. The Integrated Forecasting System (IFS) was run at TL1279 (18 km, 137 levels to 0.01 hPa, 2016 version) in its analysis (AN) and forecast (FC) modes. As the main goal of the paper is to test the operational ability of the CIMA Research Foundation hydro-meteorological chain in producing a skilful forecast of the flooding event, in the first place, the IFS FC products were used to force the model. Four experiments were performed using the four microphysical schemes introduced above. The experiments are named FC-W, FC-G, FC-T, and FC-Y for the WSM6, Goddard, Thompson, and Milbrandt-Yau schemes, respectively.

As a further step, to test the quality of the IFS-FC product and to study the sensitivity of the runs to the choice of the microphysical scheme using better initial and boundary conditions, also the IFS-AN products were used to force the same four simulations. Following the naming procedure used for the IFS-FC-driven experiments, the IFS-AN-driven ones are called AN-W, AN-G, AN-T, and AN-Y. All the simulations were initialised at 00 UTC on the 4th of November 1994 and ended at 00 UTC on the 7th of November 1994.

2.2 RainFARM model

RainFARM, the Rainfall Filtered AutoRegressive Model (Rebora et al. 2006), is a stochastic rainfall downscaling model used to generate an ensemble of high-resolution precipitation fields consistent with the large-scale predictions issued by meteorological models (Laiolo et al. 2014) and/or by expert forecasters (Silvestro et al. 2011). Such a model is needed to force the hydrological model, which runs on grid with spacing of the order of few hundreds metres (roughly 480 m in this work), with the NWP model outputs, which are generally given on grids with $O(1-10$ km) horizontal spacing (1.5 km in the present work, with reliable features starting from, at least, 6 km). The stochastic approach is introduced to account for the uncertainties in the numerical models (lateral conditions, parameterisations, and approximations in the equations of motion) and in the downscaling procedure. RainFARM is able to generate small-scale rainfall fields that consider not only the total amount of precipitation predicted by the meteorological model, but also its linear correlation structure and the position of the main rainfall patterns. Due to the straightforward link between the model parameters and the large-scale field, this model is suitable for operational downscaling procedures.

RainFARM propagates the spectral information of the large-scale meteorological predictions to smaller scales, in order to generate fine-resolution precipitation fields, that are consistent with radar observations of mid-latitude precipitation events. The basic idea is to reconstruct the Fourier spectrum of the precipitation field at small scales by preserving the NWP model information at the scales where the meteorological prediction is reliable. The rainfall field is seen as the superposition of a finite number of harmonics with decreasing amplitudes as spatial and temporal scales become smaller. Once the reliable spatial and temporal scales of the NWP model are identified (S_{rel} and T_{rel} , respectively), RainFARM produces a set of downscaled rainfall fields that are forced to preserve both the spatio-temporal patterns and the precipitation volume at these scales. For further details on the algorithm behind RainFARM, the reader is referred to Rebora et al. (2006).

In the present work, the downscaling was applied to the WRF model outputs assuming $S_{rel} = 15$ km and $T_{rel} = 6$ h. Since, from the hydrological point of view, we considered the streamflow forecast on sub-basins with relatively large drainage areas ($> 10^3$ km²), the

number of the stochastic ensemble members was kept relatively low, namely 6, because over such drainage areas small-scale variations in the precipitation distribution do not affect the hydrological forecast.

2.3 Continuum model

Continuum (Silvestro et al. 2013) is a continuous distributed hydrological model that strongly relies on a morphological approach based on a novel way for the identification of the drainage network components (Giannoni et al. 2000). Continuum is a compromise between empirical models, which are easy to implement but sometimes lack realistic features, and complex physically based models, which try to reproduce all the hydrological processes in detail, heavily relying on parameterisations. Their main drawback is that such parameterisations may introduce large uncertainties, especially when observations are sparse, which results in a non-robust estimate of the parameters.

The Continuum model has been developed keeping the rigorous physical description of the hydrological processes as simple as possible. This resulted in good performances, comparable to existing models, with an increased computational efficiency. In particular, the reduced complexity of the mathematical modelling and the relatively small number of parameters lead to a considerably lower calibration effort, increasing model robustness and portability to data-scarce environments. Thanks to the increased efficiency of the code, Continuum can be easily implemented in an ensemble configuration, enabling the modeller to directly estimate the prediction uncertainties.

The model is able to reproduce the spatio-temporal evolution of soil moisture, energy fluxes, surface soil temperature, and evapotranspiration. Moreover, it can account for the vegetation seasonal variability in terms of interception and evaporation. Deep flow and water table evolution are modelled with a simple scheme that reproduces the main physical characteristics of the processes, while a distributed interaction between water table and soil surface is represented with a simple parameterisation. The introduction of the so-called force-restore equation for the surface energy balance allows the calculation of the land surface temperature, which can be used for calibration and/or assimilation of remote sensing data.

In this work, Continuum was configured as in Davolio et al. (2017) over the upper part of the Po River basin, with a grid spacing of 0.005° (about 480 m) and a time resolution of 1 h. The results, shown in the next section, are presented in terms of stage discharge curves of four station level sections out of the seven sections modelled, that are indicated in the map of Fig. 4.

3 Results

3.1 Atmospheric model results

The WRF model outputs of the hindcast simulations run in operational mode, i.e. forced with the IFS-FC products, are shown in Fig. 5 for all four configurations (panels a–d). In particular, the maps of the accumulated rainfall over 3 days (between the 4th and the 7th of November 1994) are shown. In the same figure, in panel e, the rainfall measured by the rain gauge networks operated by ARPA Piemonte and ARPAL is shown, accumulated over the same time period. This observational network was composed, at the time of the event, by roughly 150 rain gauges, with an average inter-distance of 15 km.

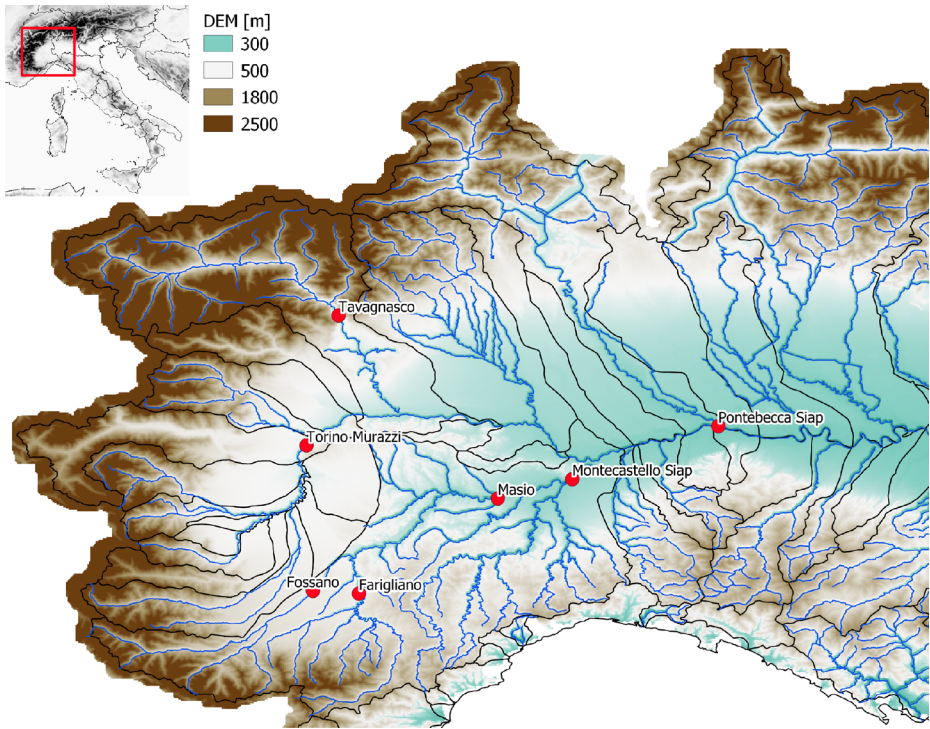


Fig. 4 Study domain of the Continuum model. The main sub-basins are drawn in black and the river network in blue. Red dots indicate the level gauges considered in the study

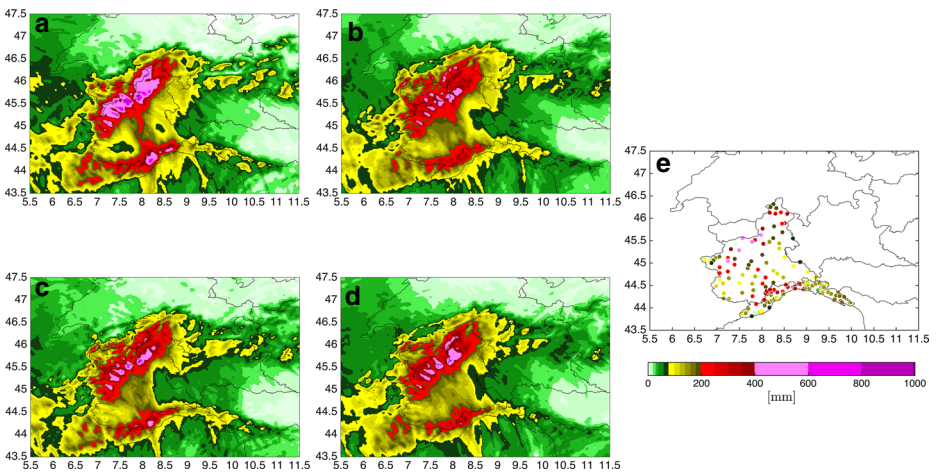


Fig. 5 Maps of the 72 h accumulated QPF for FC-W (panel a), FC-T (panel b), FC-G (panel c), FC-Y (panel d), and of the rain gauge QPE (panel e) between 00 UTC of the 4th of November and 00 UTC of the 7th of November 1994

Qualitatively, all the model configurations produced a forecast in very good agreement with the observed rainfall field. In fact, they all simulated two areas of intense rainfall located over the western part of the boundary between Piedmont and Liguria (corresponding to the Tanaro catchment area) and in northern Piedmont.

Concerning the area in northern Piedmont, all the simulated fields show the accumulated rainfall peaks in the same locations, suggesting that it was indeed the geometry of the orographic barrier to determine the air ascent and, thus, the precipitation location. In terms of differences produced by the choice of the microphysical parameterization, only the WSM6 scheme (FC-W, panel a) stood out, producing a more intense precipitation field, which can not be ascribed to the fact that WSM6 is a single-moment scheme. In fact, the experiment FC-G, which was also run with a single-moment scheme with the same hydrometeors as WSM6, produced a rainfall field that is very similar to those of the FC-T and FC-Y runs, which are both based (at least partially) on a double-moment approach.

It is worth noticing that with respect to the numerical simulations that were performed in the years following the event, such as in Buzzi et al. (1998) and in Ferretti et al. (2000), the maxima of precipitation that occurred along the maritime Alps were here reproduced in a better way. In fact, both Buzzi et al. (1998) and Ferretti et al. (2000), that used domains with 10- to 30-km grid spacing, simulated these maxima on the southern side of the mountain chain and not on the northern one, as observed. Also Buzzi and Foschini (2000), that used a 4-km grid spacing setup with parameterized convection, were not able to correctly place the rainfall over the northern side of the maritime Alps. The fact that all the configurations of this study were able to model these rainfall maxima on the correct side of the maritime Alps suggests that it is the finer resolution associated with explicit convection that allowed for a correct rainfall spatial distribution. Note that also the good quality of the initial and boundary conditions may have contributed to the improved skills of the forecast simulations. The correct rainfall spatial distribution significantly impacts the hydrological forecast, as discussed in the following section.

To validate the atmospheric modelling experiments in a quantitative way, the Quantitative Precipitation Forecast (QPF) of WRF was compared with the rain gauge Quantitative Precipitation Estimate (QPE) by using the Method for Object-Based Evaluation (Davis et al. 2006a, b, MODE) tool. MODE identifies precipitation structures in both forecast and observed fields according to a selected threshold on the accumulated rainfall field. By calculating a set of geometrical indices of the observed and forecast objects, listed in Table 1, MODE is able to perform a spatial evaluation of the model capability to reproduce the identified observed objects. As indicated in the table, MODE indices measure, for example, the objects' relative position, their relative orientation, and overlap.

To calculate the MODE indices, both the observed and the simulated rainfall fields have to be on the same grid. Since the rain gauges are distributed with an average inter-distance of roughly 14 km, both the rain gauge QPE and the QPF of innermost domain were regridded on the 13.5-km model grid with a nearest-neighbour approach. The MODE tool was used with a 216-mm threshold, corresponding to a rainfall intensity of 3 mm/h for 72 h. MODE highlighted two main distinct clusters, as previously observed: the first one over the Tanaro basin (cluster 1) and the second one over northern Piedmont (cluster 2). As an example, Fig. 6 shows the main clusters identified by MODE in the observations and in the FC-W experiment.

All the spatial indices calculated by MODE for the two clusters are summarised in Table 2. Concerning the centroid distance for cluster 1, the best performing run is FC-Y

Table 1 Names and descriptions of the MODE geometrical indices

Indices	Description
CENTROID DIST	It provides a quantitative sense of the spatial displacement of the forecast with respect to the observation (Best score: 0).
ANGLE DIFF	For non-circular objects, it gives a measure of the orientation errors (Best score: 0).
AREA RATIO	It is an objective measure of whether there is an over- or under-prediction of the areal extent of the forecast (Best score: 1).
INTERSECTION AREA	It is the area of the intersection between corresponding objects (Best score: the highest value).
UNION AREA	Sum of the INTERSECTION AREA and the non-overlapping remaining area of the two corresponding objects (Best score: the lowest value).
SYMMETRIC DIFF	Difference between the UNION AREA and the INTERSECTION AREA, it provides a good summary metric for how well the two objects match (Best score: 0).
P90 RATIO	It is the ratio of the near-peak (90th percentile) intensities found in the two objects (Best score: 1).

with a mismatch in the centroid position of about 14 km. The other experiments have a centroid displacement lower than 27 km (FC-T), which is a very good value considering that the rain gauge inter-distance is roughly 13.5 km. Similar comments hold for cluster 2, where the best performing experiment is FC-Y with a centroid distance of about 19 km and the remaining experiments have a centroid distance lower than 20.5 km. The FG-G experiment has the best performance in terms of angle difference for cluster 1 and the FC-T experiment for cluster 2. The best area ratio is reached by FC-T for both clusters, meaning that it is the setup that models at best the extent of the rainfall area. The FC-G experiment shows the strongest agreement between the observed and the predicted near-peak (90th percentile) rainfall depth in cluster 1, corresponding to the Tanaro catchment, while FC-Y does so for cluster 2, corresponding to the northern Piedmont area.

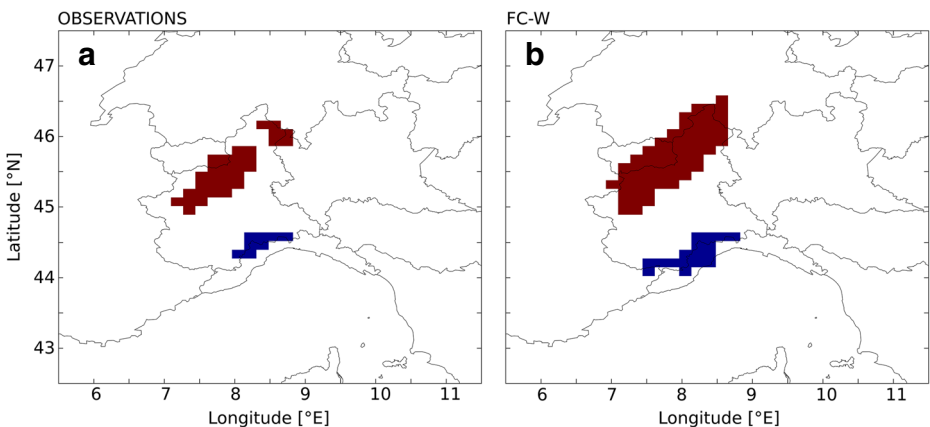


Fig. 6 Main clusters (blue: cluster 1 over the Tanaro region, red: cluster 2 over northern Piedmont) found by the MODE tool in the observed rainfall field (panel a) and in the FC-W experiment (panel b)

Table 2 Spatial indices calculated by MODE (216-mm rainfall depth threshold), with their units in square brackets. The best performance for each score for a given cluster is italicised

Run	Cluster	CENTROID DIST [km]	ANGLE DIFF [°]	AREA RATIO [1]	SYMMETRIC DIFF [km ²]	INTERSECTION AREA [km ²]	UNION AREA [km ²]	P90 RATIO [1]
FC-W	1	24.44	3.87	2.12	1640	1458	3098	1.75
FC-G	1	26.20	8.35	1.25	1458	911	2369	<i>1.01</i>
FC-T	1	27.68	13.57	<i>1.12</i>	1640	729	2369	1.35
FC-Y	1	<i>13.91</i>	12.61	0.63	<i>911</i>	729	<i>1640</i>	1.18
FC-W	2	20.25	5.13	1.94	7290	4921	12,211	1.25
FC-G	2	20.52	8.04	1.94	7655	4739	12,393	0.86
FC-T	2	19.44	4.85	<i>1.62</i>	6197	4556	<i>10,753</i>	1.04
FC-Y	2	<i>19.31</i>	6.58	1.69	7290	4192	11,482	<i>0.99</i>

Table 3 Short-duration rainfall annual maxima (mm) produced during the Piedmont 1994 event in five western-central stations in Liguria over different accumulation intervals

Duration (h)	1	3	6	12	24
Sanda	47	96.0	120.0	140.2	159.4
Sciarborasca	57	93.2	111.0	132.2	143.4
Lerca	29.4	65.6	79.6	102.6	108.0
Fiorino	87.0	114.0	142.2	175.6	190.8
Mele	60.0	116.8	160.0	199.8	211.8

As described in the “Introduction”, according to the Molini et al. (2011) criterion, severe rainfall events in the Mediterranean area can be classified in two categories: type I that are long-lived and widespread events and type II that are short and localised. The Piedmont 1994 case study was a type-I event, as indicated by the Monte Lema radar data (see Fig. 2), which show that the northern Piedmont Alpine arc was struck by persistent rain for roughly 2 days. However, as highlighted by previous works, such as Boni et al. (1996), the event was also characterised by intense convective activity, especially over central-western Liguria. This is confirmed by the fact that, in this area, the annual maxima of short-duration rainfall (accumulated over 1, 3, 6, 12, and 24 h) were attained during this event. Table 3 shows their values for five selected stations over western-central Liguria (as indicated by the black dots in Fig. 7). Note that in Fiorino the hourly accumulated rainfall maximum almost reached the exceptional value of 90 mm.

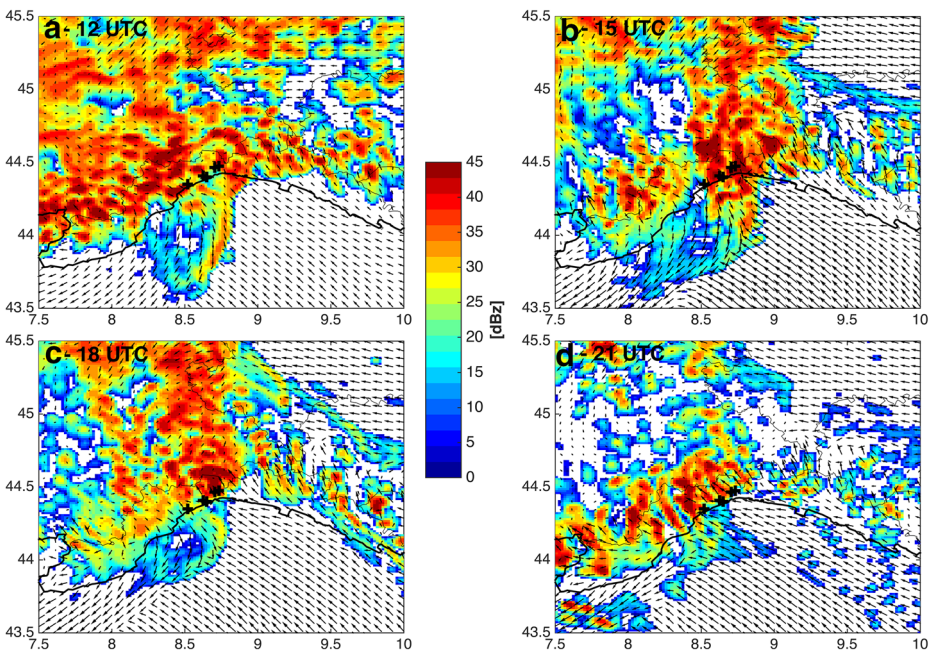


Fig. 7 VMI maps at 12, 15, 18, and 21 UTC on the 4th of November 1994 (FC-W experiment). The black markers show the position of the five stations whose short-duration rainfall annual maxima are reported in Table 3

To gain a deeper understanding of the physical mechanisms responsible for this observational evidence, the FC-W experiment was further analysed, since it is the operational setup used at CIMA. The reflectivity vertical maximum intensity (VMI) field was mapped every 3 h between 12 and 21 UTC on the 4th of November 1994, together with the 10-m wind field. The different panels of Fig. 7 show the generation and the dissipation over the Ligurian Sea of a very localised and intense convective rainfall structure known as back-building mesoscale convective system (MCS). In particular, a well-defined surface convergence line between a cold northerly wind and a warmer south-easterly flow formed at 12 UTC (panel A). This was accompanied by an elongated structure of high VMI, that is generally indicative of intense convection. In the following hours, the interaction between the surface circulation and the slow-evolving large-scale dynamics forced the convective cells to develop in the same position for few hours, as indicated by the area of maximum VMI over mid-western Liguria at 15 UTC and 18 UTC (panels b and c). It is because of this dynamical feature that this kind of systems produces very high rainfall rates and they are called “back-building”. Finally, at 21 UTC (panel D), the convergence line over the sea completely disappeared and the convective activity inland diminished significantly.

These back-building MCSs are known to hit many regions of the Mediterranean, as southern France (Ducrocq et al. 2014; Nuissier et al. 2008), northern Italy (Fiori et al. 2014; Fiori et al. 2017; Lagasio et al. 2017), and eastern Spain (Millán et al. 1995; Pastor et al. 2010), to cite some. There is evidence that they have always been a meteorological hazard in this region (Parodi et al. 2017), and that their frequency is expected to increase because of climate change effects (Gallus et al. 2018). They generally develop over the sea (Nuissier et al. 2008; Fiori et al. 2014), which has been shown to strongly affect (1) the intensity of the precipitation through its mean sea surface temperature (SST) value (Lebeauupin et al. 2006; Pastor et al. 2001; Meroni et al. 2018b), and (2) the location of the rainfall band through the horizontal variations of SST (Meroni et al. 2018a; Cassola et al. 2016).

To conclude the meteorological result section, a qualitative discussion on the outputs of the IFS-AN-driven experiments (shown in Fig. 8) is done. In particular, all the

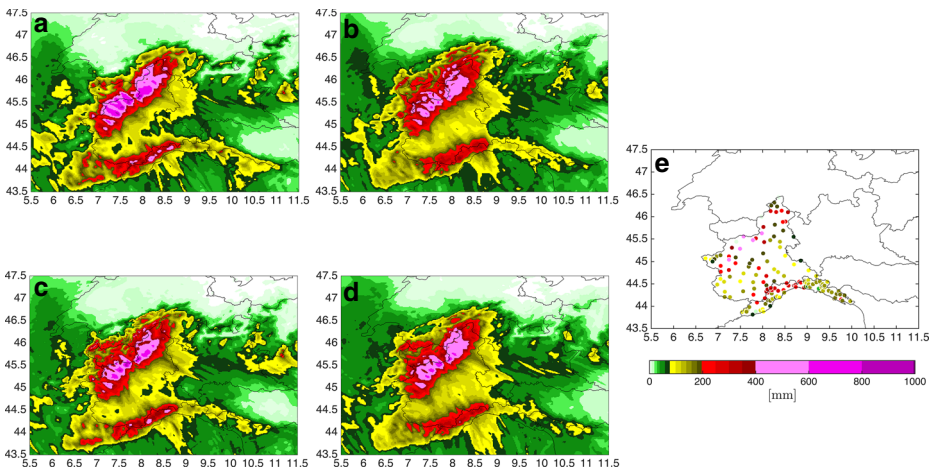


Fig. 8 Maps of the 72 h accumulated QPF for AN-W (panel a), AN-T (panel b), AN-G (panel c), AN-Y (panel d), and of the rain gauge QPE (panel e) between 00 UTC of the 4th of November and 00 UTC of the 7th of November 1994

configurations produced a rainfall field in agreement with the observations, with a higher simulated rainfall volume with respect to the IFS-FC-driven experiments. WSM6 was the one that produced, once again, the highest accumulated rainfall values. This suggests that it is indeed the numerical scheme to generate a higher value of rainfall. However, the differences among the IFS-FC-driven experiments and among the IFS-AN-driven ones are smaller than the difference between the IFS-FC run and the corresponding IFS-AN one for a given setup. This confirms that, as previously discussed, this event was strongly driven by the large-scale conditions (especially for the northern Piedmont area). Thus, by changing the initial and boundary conditions (from IFS-FC to IFS-AN), larger differences are introduced with respect to changing the numerical description of the microphysical processes.

The added value of the IFS-AN runs might be seen in the convective rain phase that hit the mid-western part of Liguria. In fact, all the IFS-AN runs produced a similar v-shape pattern over the sea (which is almost touching the southern border of the figure, at around 9° E) of accumulated rainfall above roughly 80 mm (yellow shading in Fig. 8), which is characteristic of the back-building MCSs, as discussed above. In the IFS-FC-driven runs (Fig. 5), instead, the four configurations produced different elongated rain bands, with rainfall covering larger areas with a weaker intensity, suggesting that the large-scale conditions were not properly driving the atmospheric dynamics in the generation of the back-building MCS.

3.2 Hydrological model results

The hydrological chain was then applied starting from all the IFS-FC experiments, simulating an operational framework. The simulated rainfall fields were downscaled to the Continuum grid using RainFARM, as discussed in Section 2.2. The results in terms of peak flow prediction are summarised in Table 4 in which the following quantities are reported:

- The observed peak (only the peak estimates were available (Piemonte 1998));
- The peak flow of the hydrological modelling fed with the observed rainfall field (named “Run Observation”);
- The minimum and maximum peak discharge values from the hydrological ensembles of each rainfall forecast.

Table 4 Data for all FC experiments. *Qobs* are the observations; *Qsim* corresponds to the peaks obtained from the Run Observation. *QForecastMax* and *QForecastMin* are the maximum and minimum peak values obtained from each FC experiment. All quantities are in $m^3 s^{-1}$

Run	QForecastMax	QForecastMin	Fossano	Monte Castello	Tavagnasco	Torino
Qobs	-	-	900	4200	1100	1800
Qsim	-	-	980	3800	750	1750
FC-W	Max	-	2300	5500	2500	2300
	Min	-	2000	5000	2000	2000
FC-G	Max	-	1400	5200	4000	1500
	Min	-	1200	4000	3200	1400
FC-T	Max	-	1500	4300	2900	1800
	Min	-	1200	3600	2400	1600
FC-Y	Max	-	1200	4800	3800	1500
	Min	-	1000	4100	3300	1400

All the analyses were performed on the seven stations presented in Fig. 4. Here, for the sake of brevity, the results of four representative stations opportunely chosen are reported: Fossano and Monte Castello are chosen for cluster 1 (Tanaro basin), while Tavagnasco and Torino stations are chosen for cluster 2 (northern Piedmont). In Fig. 9, the hydrographs for the same four-level gauges are shown. Note that at the time of the event, no official hydrological forecast was available.

The Run Observation experiment (black lines with empty circles) reproduced quite well the observed peak flows (full red circles) in the selected sections. The sources of error can generally be related to the uncertainties of the hydrological modelling, such as the parameterisations and the soil moisture initial conditions, and to a bad representation of the rainfall input over part of the basin. This was indeed the case, as the rain gauge stations used to generate the interpolated rainfall maps were not very dense, meaning that the rainfall pattern was not very well represented. The Run Observation experiment in the Tavagnasco and Monte Castello sections evidenced a low underestimation of the observed peak discharge, while for Torino and Fossano sections, the simulations were good.

Concerning the FC experiments, on the Tavagnasco station, all the configurations overestimated the peak discharge, probably because the simulated rainfall exceeded the observations in northern Piedmont (cluster 2). The FC-W experiment had the best performances on the Tavagnasco section, while it slightly overestimated the peak flows on Torino, Fossano, and Monte Castello with all members. This overestimation can be probably ascribed to the larger amount of rainfall predicted by FC-W simulation over cluster 1 (refer to panel a of Fig. 5). The FC-G showed good skills from an early warning perspective on Torino and Monte Castello sections for all members. The best performances in cluster 1 sections were achieved by FC-T and FC-G, which both produced a good forecast in an early warning perspective. The good agreement between the Run Observation peak flow forecast (black lines with empty circles) and the actual observed peak flow values (full red circles)

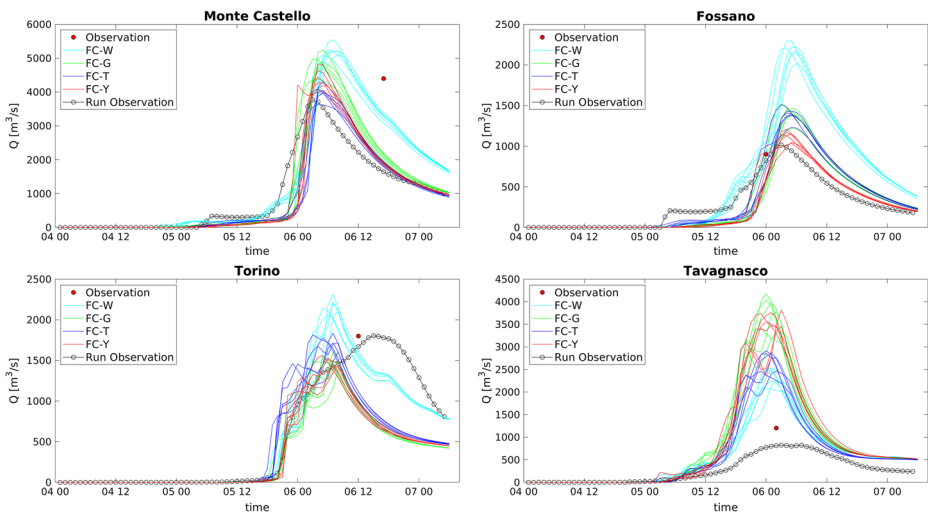


Fig. 9 Results for four level gauges. The red dots indicate the observed peak flow values; the black lines with empty circles are the results of the Run Observation experiments and the continuous lines are the forecast scenarios for the six members of each FC experiment

suggests that the hydrological model was correctly calibrated and it was reliable on the analysed sections. The mismatch between FC runs and the peak flow observations, thus, can be mainly ascribed to the uncertainties in the location and intensity of the rainfall prediction. In fact, neither a bad positioning of the rainfall field on spatial scales larger than S_{rel} nor large errors in the accumulated rainfall depth can be managed by the downscaling algorithm.

Concerning the forecast timing, in Monte Castello and Torino, all the simulated peak flows preceded the observed ones (in Monte Castello, this holds also for the Run Observation experiment), but they would still be good to issue a warning. A very good timing was reported for Fossano, which had just a slight delay, and Tavagnasco section, characterised by a peak discharge overestimation. Globally, in an early warning system perspective, even with some uncertainties in the peak timing and intensity, all the FC experiments revealed very good performances and they would have led to issue an alert. This is particularly relevant for the sections hit by cluster 1 (Monte Castello and Fossano), because, as already discussed in the previous section, past numerical works were not able to correctly place the heavy rainfall of cluster 1 on the northern side of the Ligurian Alps, which would have led to completely miss the strong hydrological response.

4 Conclusions

The CIMA Research Foundation operational hydro-meteorological forecasting chain, driven by ECMWF-IFS forecast products, and including a cloud-resolving NWP model (WRF), a stochastic rainfall downscaling model (RainFARM), and a continuous distributed hydrological model (Continuum), has been used to study the Piedmont and Liguria 1994 HPE from its meteorological onset to the hydrological effects.

In particular, the WRF model has been run mimicking an operational setup at cloud-resolving grid spacing. A multi-physics approach adopting four different microphysical schemes was pursued. The chosen parameterisations include both single-moment and double-moment schemes. Indeed, all the IFS-FC-driven experiments run with WRF correctly reproduced the rainfall structure of the event. In particular, they had very good predicting skills, both thanks to the high quality of the IFS-FC products and because the event was driven by the large-scale dynamics. The evident improvement introduced with the use of the high resolution and the explicit convection is found in the convective phase of the event that hit western Liguria on the 4th of November 1994. In fact, firstly, a proper localisation of the rainfall area over the northern side of the Maritime Alps is obtained, which was not the case in previous works. Secondly, a convincing back-building MCS is produced in the simulations, in agreement with the extreme values of short-duration accumulated rainfall observed by various Ligurian rain gauges.

Comparisons with the simulations driven by the ECMWF-IFS analysis products confirm the relevance of the large-scale forcing in this event, highlighting that changing the microphysical scheme does not lead to significant variations in the forecast.

Indeed, the four FC experiments have been used in the hydrological chain built with RainFARM and Continuum hydrological models. This was done to assess the impact of the different WRF configurations in terms of peak discharge forecast. It was found that the hydro-meteorological chain was able to properly describe the observed discharge peak. Despite some uncertainty in the peak timing and intensity, the CIMA Research Foundation chain applied to all the FC experiments would have led to an alert in an early warning system framework. The hydrological results did not appear to depend on the choice of the microphysical scheme in the atmospheric model. This happened because the rainfall field

was mainly controlled by the large-scale forcing, as discussed above. Since, at the time of the event, no official hydro-meteorological early warning system was in place, these results are very relevant to show the importance for the society of an appropriate high-resolution hydro-meteorological chain.

As mentioned before, the WRF modelling experiments have highlighted the occurrence of a back-building MCS on the 4th of November, in good agreement with the short-duration rainfall annual maxima detected on the same day over western Liguria. These back-building MCSs often hit the Liguria region, and many other parts of the Mediterranean basin, during autumn and are triggered by a convergence line over the sea. Despite the back-building MCSs often develop within large-scale synoptic disturbances, as happened in the November 1994 case, they might also develop in nearly clear-sky conditions (Fiori et al. 2017; Lagasio et al. 2017). The different large-scale conditions in which these phenomena develop are tightly linked to their predictability. In fact, in the latter case, local and small-scale forcing factors are responsible for the convection development, meaning that a good forecast is much harder to produce. For this reason, research is still very active in trying to improve the forecast of such short-lived and highly localised events, in terms of rainfall amount, localisation, and timing. Work is ongoing towards the future operational use of a hydro-meteorological framework coupling a high-resolution NWP model, including data assimilation of high-resolution satellite observations (Lagasio et al. 2019a; Meroni et al. 2020), possibly in nowcasting mode, with hydrological modelling, to further improve the peak discharge forecasts.

Work is ongoing to support the findings of the present study, which was performed over a single heavy rainfall event, in terms of the forecast skills of the CIMA hydro-meteorological chain. In particular, the authors are involved in a new work with a more robust set of statistics to show that the above-mentioned forecasting chain is skilful throughout the year over the entire Italian country. Using a fuzzy-logic approach, the rainfall intensity and the spatial scales over which the forecasting chain is reliable are being studied and will be the object of a future publication.

Acknowledgements We acknowledge the Italian Civil Protection Department, ARPA Piemonte, and ARPA Liguria for providing the Italian Weather Stations Network data. We are also grateful to MeteoSwiss for the Monte Lema radar maps. Thanks are due to LRZ Supercomputing Centre, Garching, Germany, where the numerical simulations were performed on the SuperMUC Petascale System, Project-ID: pr62ve. A. N. M. acknowledges support from the TWIGA project, which has received funding from the European Union's Horizon 2020 Research and Innovation Programme under grant agreement No.776691.

Compliance with ethical standards

Conflict of interest The authors declare that they have no conflict of interest.

Open Access This article is licensed under a Creative Commons Attribution 4.0 International License, which permits use, sharing, adaptation, distribution and reproduction in any medium or format, as long as you give appropriate credit to the original author(s) and the source, provide a link to the Creative Commons licence, and indicate if changes were made. The images or other third party material in this article are included in the article's Creative Commons licence, unless indicated otherwise in a credit line to the material. If material is not included in the article's Creative Commons licence and your intended use is not permitted by statutory regulation or exceeds the permitted use, you will need to obtain permission directly from the copyright holder. To view a copy of this licence, visit <http://creativecommons.org/licenses/by/4.0/>.


References

- Boni G, Conti M, Dietrich S, Lanza L, Marzano FS, Mugnai A, Panegrossi G, Siccardi F (1996) Multisensor observations during the flood event of 4–6 November, 1994 over Northern Italy. *Remote Sens Rev* 14(1–3):91–117. <https://doi.org/10.1080/02757259609532314>
- Bougeault P, Binder P, Buzzi A, Dirks R, Houze R, Kuettner J, Smith RB, Steinacker R, Volkert H (2001) The MAP special observing period. *Bull Amer Meteor Soc* 82(3):433–462
- Buzzi A, Foschini L (2000) Mesoscale meteorological features associated with heavy precipitation in the southern Alpine region. *Meteor Atm Phys* 72:131–146
- Buzzi A, Tartaglione N, Malguzzi P (1998) Numerical simulations of the 1994 Piedmont flood: role of orography and moist processes. *Mon Weather Rev* 126:2369–2383
- Cassola F, Ferrari F, Mazzino A, Miglietta MM (2016) The role of the sea in the flash floods events over Liguria (northwestern Italy). *Geophys Res Letters* 43:3534–3542. <https://doi.org/10.1002/2016GL068265>
- Chiao S, Lin YL, Kaplan ML (2004) Numerical study of the orographic forcing of heavy precipitation during MAP IOP-2B. *Mon Weather Rev* 132(9):2184–2203. [https://doi.org/10.1175/1520-0493\(2004\)132<2184:NSOTOF>2.0.CO;2](https://doi.org/10.1175/1520-0493(2004)132<2184:NSOTOF>2.0.CO;2)
- Davis AC, Brown B, Bullock R (2006a) Object-based verification of precipitation forecasts. Part I: methodology and application to mesoscale rain areas. *Mon Weather Rev* 134:1772–1784. <https://doi.org/10.1175/MWR3145.1>
- Davis AC, Brown B, Bullock R (2006b) Object-based verification of precipitation forecasts. Part II: application to convective rain system. *Mon Weather Rev* 134:1785–1795. <https://doi.org/10.1175/MWR3146.1>
- Davolio S, Silvestro F, Galardo T (2017) Impact of rainfall assimilation on high-resolution hydrometeorological forecasts over Liguria, Italy. *J Hydromet* 18(10):2659–2680
- Dayan U, Nissen K, Ulbrich U (2015) Review article: Atmospheric conditions inducing extreme precipitation over the eastern and western Mediterranean. *Nat Hazards Earth Sys Sci* 15:2525–2544. <https://doi.org/10.5194/nhess-15-2525-2015>
- Doswell III CA, Ramis C, Romero R, Alonso S (1998) A diagnostic study of three heavy precipitation episodes in the western Mediterranean region. *Weather Forecast* 13:102–124
- Ducrocq V, Braud I, Davolio S, Ferretti R, Flamant C, Jansa A, Kalthoff N, Richard E, Taupier-Letage I, Ayrat PA, et al. (2014) Hymex-sop1: the field campaign dedicated to heavy precipitation and flash flooding in the northwestern Mediterranean. *Bull Amer Meteor Soc* 95(7):1083–1100
- Ferretti R, Low-Nam S, Rotunno R (2000) Numerical simulations of the Piedmont flood of 4–6 November 1994. *Tellus A* 52:162–180. <https://doi.org/10.3402/tellusa.v52i2.12261>
- Fiori E, Comellas A, Molini L, Rebora N, Siccardi F, Gochis D, Tanelli S, Parodi A (2014) Analysis and hindcast simulations of an extreme rainfall event in the Mediterranean area: the Genoa 2011 case. *Atmos Res* 138:13–29
- Fiori E, Ferraris L, Molini L, Siccardi F, Kranzlmüller D, Parodi A (2017) Triggering and evolution of a deep convective system in the Mediterranean Sea: modelling and observations at a very fine scale. *Q J R Meteor Soc* 143(703):927–941. <https://doi.org/10.1002/qj.2977>
- Gallus Jr, W A, Parodi A, Maugeri M (2018) Possible impacts of a changing climate on intense Ligurian Sea rainfall events. *Int J Climatol* 38:e323–e329
- Giannoni F, Roth G, Rudari R (2000) A semi-distributed rainfall-runoff model based on a geomorphologic approach. *Physics and Chemistry of the Earth, Part B: Hydrology, Oceans and Atmosphere* 25(7–8):665–671
- Hong SY, Lim JOJ (2006) The wrf single-moment 6-class microphysics scheme (wsm6). *J Korean Meteor Soc* 42(2):129–151
- Hong SY, Noh Y, Dudhia J (2006) A new vertical diffusion package with an explicit treatment of entrainment processes. *Mon Weather Rev* 134(9):2318–2341
- Iacono MJ, Mlawer EJ, Clough SA, Morcrette JJ (2000) Impact of an improved longwave radiation model, RRTM, on the energy budget and thermodynamic properties of the NCAR community climate model, CCM3. *J Geophys Res Atmos* 105(D11):14873–14890
- Iacono MJ, Delamere JS, Mlawer EJ, Shephard MW, Clough SA, Collins WD (2008) Radiative forcing by long-lived greenhouse gases: calculations with the AER radiative transfer models. *J Geophys Res Atmos* 113(D13)
- Lagasio M, Parodi A, Procopio R, Rachidi F, Fiori E (2017) Lightning Potential Index performances in multimicrophysical cloud-resolving simulations of a back-building mesoscale convective system: the Genoa 2014 event. *J Geophys Res Atmos* 122(8):4238–4257. <https://doi.org/10.1002/2016JD026115>

- Lagasio M, Parodi A, Pulvirenti L, Meroni AN, Boni G, Pierdicca N, Marzano FS, Luini L, Venuti G, Realini E, et al. (2019a) A synergistic use of a high-resolution numerical weather prediction model and high-resolution earth observation products to improve precipitation forecast. *Remote Sens* 11(20):2387
- Lagasio M, Pulvirenti L, Parodi A, Boni G, Pierdicca N, Venuti G, Realini E, Tagliaferro G, Barindelli S, Rommen B (2019b) Effect of the ingestion in the WRF model of different Sentinel-derived and GNSS-derived products: analysis of the forecasts of a high impact weather event. *Eur J Remote Sens* 52(sup4):16–33
- Lagasio M, Silvestro F, Campo L, Parodi A (2019c) Predictive capability of a high-resolution hydrometeorological forecasting framework coupling WRF cycling 3dvar and Continuum. *J Hydromet* 20(7):1307–1337
- Laiolo P, Gabellani S, Rebora N, Rudari R, Ferraris L, Ratto S, Stevenin H, Cauduro M (2014) Validation of the flood-proofs probabilistic forecasting system. *Hydrol Processes* 28(9):3466–3481
- Lebeaupin C, Ducrocq V, Giordani H (2006) Sensitivity of torrential rain events to the sea surface temperature based on high-resolution numerical forecasts. *J Geophys Res Atmos* 111(D12)
- Lionetti M (1996) The Italian floods of 4–6 November 1994. *Weather* 51:18–27
- Llasat MC, Llasat-Botija M, Petrucci O, Pasqua AA, Rosselló J, Vinet F, Boissier L (2013) Towards a database on societal impact of mediterranean floods within the framework of the hymex project. *Nat Hazards Earth Sys Sci* 13:1337–1350. <https://doi.org/10.5194/nhess-13-1337-2013>
- Marras I, Fiori E, Rossi L, Parodi A (2017) Effects of the representation of convection on the modelling of hurricane Tomas (2010). *Adv Meteor*:2017. <https://doi.org/10.1155/2017/1762137>
- McCumber M, Tao WK, Simpson J, Penc R, Soong ST (1991) Comparison of ice-phase microphysical parameterization schemes using numerical simulations of tropical convection. *J Appl Meteor* 30(7):985–1004
- Meroni AN, Parodi A, Pasquero C (2018a) Role of SST patterns on surface wind modulation of a heavy midlatitude precipitation event. *J Geophys Res Atmos* 123:9081–9096. <https://doi.org/10.1029/2018JD028276>
- Meroni AN, Renault L, Parodi A, Pasquero C (2018b) Role of the oceanic vertical thermal structure in the modulation of heavy precipitations over the Ligurian Sea. *Pure Appl Geophys* 175:4111–4130. <https://doi.org/10.1007/s00024-018-2002-y>
- Meroni AN, Montrasio M, Venuti G, Barindelli S, Mascitelli A, Manzoni M, Monti Guarnieri A, Gatti A, Lagasio M, Parodi A, Realini E, Tagliaferro G (2020) On the definition of the strategy to obtain absolute InSAR Zenith Total Delay maps for meteorological applications. *Front Earth Sci* 8:359. <https://doi.org/10.3389/feart.2020.00359>
- Milbrandt J, Yau M (2005a) A multi-moment bulk microphysics parameterization. Part I: analysis of the role of the spectral shape parameter. *JAS* 62(9):3051–3064
- Milbrandt J, Yau M (2005b) A multi-moment bulk microphysics parameterization. Part II: a proposed three-moment closure and scheme description. *JAS* 62(9):3065–3081
- Millán M, Estrela J, Caselles V (1995) Torrential precipitations on the Spanish east coast: the role of the Mediterranean sea-surface temperature. *Atmos Res* 36:1–16
- Mlawer EJ, Taubman SJ, Brown PD, Iacono MJ, Clough SA (1997) Radiative transfer for inhomogeneous atmospheres: RRTM, a validated correlated-k model for the longwave. *J Geophys Res Atmos* 102(D14):16663–16682
- Molini L, Parodi A, Rebora N, Craig GC (2011) Classifying severe rainfall events over Italy by hydrometeorological and dynamical criteria. *Q J R Meteor Soc* 137(654):148–154. <https://doi.org/10.1002/2017JD027472>
- Nuissier O, Ducrocq V, Ricard D, Lebeaupin C, Anquetin S (2008) A numerical study of three catastrophic precipitating events over southern France. I: numerical framework and synoptic ingredients. *Q J R Meteor Soc* 134:111–130. <https://doi.org/10.1002/qj.200>
- Parodi A, Tanelli S (2010) Influence of turbulence parameterizations on high-resolution numerical modeling of tropical convection observed during the TC4 field campaign. *J Geophys Res Atmos*:115(D10)
- Parodi A, Boni G, Ferraris L, Siccardi F, Pagliara P, Trovatore E, Fofoula-Georgiou E, Kranzlmüller D (2012) The “perfect storm”: from across the Atlantic to the Hills of Genoa. *Eos, Transactions American Geophysical Union* 93(24):225–226
- Parodi A, Ferraris L, Gallus W, Maugeri M, Molini L, Siccardi F, Boni G (2017) Ensemble cloud-resolving modelling of a historic back-building mesoscale convective system over Liguria: the San Fruttuoso case of 1915. *CP* 13:455–472. <https://doi.org/10.5194/cp-13-455-2017>
- Parodi A, Lagasio M, Maugeri M, Turato B, Gallus W (2019) Observational and modelling study of a major downburst event in Liguria: the 14 October 2016 case. *Atmosphere* 10(12):788
- Pastor F, Estrela MJ, Peñarocha D, Millán MM (2001) Torrential rains on the Spanish Mediterranean coast: modeling the effects of the sea surface temperature. *J Appl Meteor* 40(7):1180–1195

- Pastor F, Gómez I, Estrela MJ (2010) Numerical study of the October 2007 flash flood in the Valencia region (Eastern Spain): the role of the orography. *Nat Hazards Earth Sys Sci* 10:1331–1345. <https://doi.org/10.5194/nhess-10-1331-2010>
- Piemonte (1998) Eventi alluvionali in piemonte: 2–6 novembre 1994, 8 luglio 1996, 7-10 ottobre 1996. Direzione Servizi Tecnici di Prevenzione, Torino
- Powers JG, Klemp JB, Skamarock WC, Davis CA, Dudhia J, Gill DO, Coen JL, Gochis DJ, Ahmadov R, Peckham SE, et al. (2017) The weather research and forecasting model: overview, system efforts, and future directions. *Bull Amer Meteor Soc* 98(8):1717–1737
- Rebora N, Ferraris L, von Hardenberg J, Provenzale A (2006) RainFARM: rainfall downscaling by a filtered autoregressive model. *J Hydromet* 7(4):724–738
- Roe GH (2005) Orographic precipitation. *Annu Rev Earth Planet Sci* 33:645–671. <https://doi.org/10.1146/annurev.earth.33.092203.122541>
- Roe GH, Baker MB (2006) Microphysical and geometrical controls on the pattern of orographic precipitation. *J Atmos Sci* 63:861–880
- Romero R, Ramis C, Alonso S, Doswell III CA, Stensrud D (1998) Mesoscale model simulations of three heavy precipitation events in the western Mediterranean region. *Mon Weather Rev* 126:1859–1881
- Rotunno R, Ferretti R (2001) Mechanisms of intense alpine rainfall. *J Atmos Sci* 58:1732–1749
- Silvestro F, Rebora N, Ferraris L (2011) Quantitative flood forecasting on small-and medium-sized basins: a probabilistic approach for operational purposes. *J Hydromet* 12(6):1432–1446
- Silvestro F, Gabellani S, Delogu F, Rudari R, Boni G (2013) Exploiting remote sensing land surface temperature in distributed hydrological modelling: the example of the continuum model. *Hydrol. Earth Syst. Sci.* 17(1):39
- Silvestro F, Rossi L, Campo L, Parodi A, Fiori E, Rudari R, Ferraris L (2019) Impact-based flash-flood forecasting system: sensitivity to high resolution numerical weather prediction systems and soil moisture. *J Hydrol* 572:388–402
- Skamarock WC, Klemp JB, Dudhia J, Gill DO, Barker DM, Duda MG, Huang XY, Wang W, Powers JG (2008) A description of the advanced research WRF Version 3. NCAR Tech Note NCAR/TN-475+STR p 113. <https://doi.org/10.5065/D68S4MVH>
- Smirnova TG, Brown JM, Benjamin SG (1997) Performance of different soil model configurations in simulating ground surface temperature and surface fluxes. *Mon Weather Rev* 125:1870–1884
- Smirnova TG, Brown JM, Benjamin SG, Kim D (2000) Parameterization of cold season processes in the maps land-surface scheme. *J Geophys Res* 105(D3):4077–4086
- Tao WK, Simpson J, Baker D, Braun S, Chou MD, Ferrier B, Johnson D, Khain A, Lang S, Lynn B (2001) Microphysics, radiation and surface processes in the Goddard Cumulus Ensemble (GCE) model. *MAP* 82:97–137
- Thompson G, Field PR, Rasmussen RM, Hall WD (2008) Explicit forecasts of winter precipitation using an improved bulk microphysics scheme. Part II: implementation of a new snow parameterization. *Mon Weather Rev* 136(12):5095–5115
- Tiedtke M (1989) A comprehensive mass flux scheme for cumulus parameterization in large-scale models. *Mon Weather Rev* 117(8):1779–1800. [https://doi.org/10.1175/1520-0493\(1989\)117<1779:ACMFSF>2.0.CO;2](https://doi.org/10.1175/1520-0493(1989)117<1779:ACMFSF>2.0.CO;2)
- Viterbo F, von Hardenberg J, Provenzale A, Molini L, Parodi A, Sy O, Tanelli S (2016) High-resolution simulations of the 2010 Pakistan flood event: sensitivity to parameterizations and initialization time. *J Hydromet* 17(4):1147–1167
- Volkert H (2005) The Mesoscale Alpine Programme (MAP): a multi-faceted success story. In: Preprints ICAM/MAP 2005, Zadar, Croatia, 23–27 May 2005, pp 226–230
- Zängl G (2007a) Interaction between dynamics and cloud microphysics in orographic precipitation enhancement: a high resolution modeling study of two North Alpine heavy-precipitation events. *Mon Weather Rev* 135:2817–2840. <https://doi.org/10.1175/MWR3445.1>
- Zängl G (2007b) Small-scale variability of orographic precipitation in the Alps: case studies and semi-idealized numerical simulations. *Q J R Meteor Soc* 133(628):1701–1716. <https://doi.org/10.1002/qj.163>
- Zhang C, Wang Y, Hamilton K (2011) Improved representation of boundary layer clouds over the southeast Pacific in ARW-WRF using a modified Tiedtke cumulus parameterization scheme. *Mon Weather Rev* 139(11):3489–3513

Affiliations

Antonio Parodi¹  · **Martina Lagasio¹** · **Agostino N. Meroni^{1,2}** · **Flavio Pignone¹** · **Francesco Silvestro¹** · **Luca Ferraris¹**

Martina Lagasio
martina.lagasio@cimafoundation.org

Agostino N. Meroni
agostino.meroni@cimafoundation.com

Flavio Pignone
flavio.pignone@cimafoundation.org

Francesco Silvestro
francesco.silvestro@cimafoundation.org

Luca Ferraris
luca.ferraris@cimafoundation.org

¹ CIMA Research Foundation, Via A. Magliotto 2, Savona 17100, Italy

² Department of Civil and Environmental Engineering, Politecnico di Milano, Piazza Leonardo da Vinci, 32, 20133, Milan, Italy